Reactions of $[NEt_4][10\text{-}endo\text{-}\{Au(PPh_3)\}\text{-}nido\text{-}7,8\text{-}C_2B_9H_9Me_2]$: Carbaborane Cage Transfer from Gold to Rhodium *

John C. Jeffery,[a] Paul A. Jelliss[a] and F. Gordon A. Stone[b]

[a] *School of Chemistry, The University, Bristol BS8 1TS, UK*

[b] *Department of Chemistry, Baylor University, Waco, TX 76798-7348, USA*

The reagent $[NEt_4][10\text{-}endo\text{-}\{Au(PPh_3)\}\text{-}nido\text{-}7,8\text{-}C_2B_9H_9Me_2]$ has been prepared, and used to synthesise several mixed-metal complexes in which gold atoms are bonded to rhodium. Thus treatment of the gold salt with *trans*-$[RhCl(CO)(PPh_3)_2]$ or $[Rh_2(\mu\text{-}Cl)_2(CO)_4]$ in thf (tetrahydrofuran), in the presence of $TlBF_4$, affords the complexes $[RhAu(CO)(PPh_3)L(\eta^5\text{-}7,8\text{-}C_2B_9H_9Me_2)]$ (L = PPh_3 or CO), respectively. Reaction of the gold species with $[RhCl(PPh_3)_3]$ gives the complex $[exo\text{-}5,10\text{-}\{Rh(PPh_3)_2\}\text{-}5,10\text{-}(\mu\text{-}H)_2\text{-}10\text{-}endo\text{-}\{Au(PPh_3)\}\text{-}nido\text{-}7,8\text{-}C_2B_9H_7Me_2]$, the structure of which has been established by X-ray diffraction. The latter complex in solution exists in equilibrium with a minor isomer $[RhAu(PPh_3)_3(\eta^5\text{-}7,8\text{-}C_2B_9H_9Me_2)]$ containing a *closo*-3,1,2-RhC_2B_9 cage system. With the rhodium complex $[Rh(cod)(PPh_3)_2][PF_6]$ (cod = cycloocta-1,5-diene), and in the presence of molecular hydrogen, the gold reagent yields a chromatographically separable mixture of $[exo\text{-}5,10\text{-}\{Rh(PPh_3)_2\}\text{-}5,10\text{-}(\mu\text{-}H)_2\text{-}10\text{-}endo\text{-}\{Au(PPh_3)\}\text{-}nido\text{-}7,8\text{-}C_2B_9H_7Me_2]$ and $[RhAu_2(\mu\text{-}H)(PPh_3)_3(\eta^5\text{-}7,8\text{-}C_2B_9H_9Me_2)]$. A single-crystal X-ray diffraction study has established the structure of the rhodium–digold compound. The NMR data (^1H, $^{13}C\text{-}\{^1H\}$, $^{31}P\text{-}\{^1H\}$ and $^{11}B\text{-}\{^1H\}$) for the new compounds are reported and discussed in relation to their structures.

We have previously reported[1] several gold–rhodium compounds containing carbaborane ligands as part of a study of complexes with bonds between dissimilar metal atoms. These products have been obtained by treating various chlorogold species with the reagents $[NEt_4][Rh(CO)L(\eta^5\text{-}7,n\text{-}C_2B_9H_9R_2)]$ (n = 8 or 9, L = CO or PPh_3, R = H or Me). Thus reactions between $[AuCl(PPh_3)]$ and the salts $[NEt_4][Rh(CO)L(\eta^5\text{-}7,8\text{-}C_2B_9H_9R_2)]$ give the dimetal complexes $[RhAu(CO)(PPh_3)L(\eta^5\text{-}7,8\text{-}C_2B_9H_9R_2)]$ (R = H, L = PPh_3 **1a**; R = Me, L = PPh_3 **1b**; R = Me, L = CO **1c**).[1a,b] The corresponding reaction using $[NEt_4][Rh(CO)(PPh_3)(\eta^5\text{-}7,9\text{-}C_2B_9H_{11})]$ yields $[RhAu(CO)(PPh_3)_2(\eta^5\text{-}7,9\text{-}C_2B_9H_{11})]$ **1d**, an isomer of **1a** in which the cage CH vertices are not adjacent.[1c] More complex molecules have also been prepared. Thus the dichlorodigold compounds $[Au_2Cl_2\{\mu\text{-}Ph_2P(CH_2)_nPPh_2\}]$ (n = 2–6) with $[NEt_4][Rh(CO)(PPh_3)(\eta^5\text{-}7,9\text{-}C_2B_9H_{11})]$ afford a series of complexes $[Rh_2Au_2\{\mu\text{-}Ph_2P(CH_2)_nPPh_2\}\text{-}(CO)_2(PPh_3)_2(\eta^5\text{-}7,9\text{-}C_2B_9H_{11})_2]$ **2**,[1c] and treatment of $[WAuCl(\mu\text{-}CC_6H_4Me\text{-}4)(CO)_2(\eta\text{-}C_5H_5)]$ with $[NEt_4][Rh(CO)(PPh_3)(\eta^5\text{-}7,8\text{-}C_2B_9H_9Me_2)]$ gives a mixture of $[WRhAu(\mu\text{-}CC_6H_4Me\text{-}4)(CO)_4(\eta\text{-}C_5H_5)(\eta^5\text{-}7,8\text{-}C_2B_9H_9Me_2)]$ **3** and $[WRh_2Au_2(\mu_3\text{-}CC_6H_4Me\text{-}4)(CO)_6(\eta\text{-}C_5H_5)(\eta^5\text{-}7,8\text{-}C_2B_9H_9Me_2)_2]$ **4**.[1a]

In this paper we report a different approach to the synthesis of gold–rhodium compounds containing carbaborane groups. The new methodology is based on the isolobal mapping of the anions $[10\text{-}endo\text{-}H\text{-}nido\text{-}7,8\text{-}C_2B_9H_9R_2]^-$ and $[10\text{-}endo\text{-}\{Au(PPh_3)\}\text{-}nido\text{-}7,8\text{-}C_2B_9H_9R_2]^-$ recently highlighted by X-ray diffraction studies.[2] In these anions, isolobal H and $Au(PPh_3)$ groups[3] are *endo* σ-bonded to one boron atom in the open C_2B_3 face of the cage. Salts of the anion $[10\text{-}endo\text{-}H\text{-}nido\text{-}7,8\text{-}C_2B_9H_9Me_2]^-$ have for many years been known to react with transition-element halides to give complexes in which a metal atom is ligated by an $\eta^5\text{-}7,8\text{-}C_2B_9H_9Me_2$ group.[4] It seemed probable, therefore, that salts of $[10\text{-}endo\text{-}\{Au(PPh_3)\}\text{-}nido\text{-}7,8\text{-}C_2B_9H_9Me_2]^-$ would also be useful reagents in synthesis, affording products containing gold bonded to other metals. Herein we describe the preparation of $[NEt_4][10\text{-}endo\text{-}\{Au(PPh_3)\}\text{-}nido\text{-}7,8\text{-}C_2B_9H_9Me_2]$ **5a**, and the use of this reagent to obtain compounds with gold–rhodium bonds. A preliminary account of this work has been given.[5] The related species **5b** has been reported by Hamilton and Welch[2b] and its structure determined.

Results and Discussion

Treatment of a thf (tetrahydrofuran) solution of $Na_2[7,8\text{-}C_2B_9H_9Me_2]$ with $[AuCl(PPh_3)]$, followed by addition of $[NEt_4]Cl$, afforded the yellow salt **5a** in good yield. Data characterising this product are given in Tables 1–3. The $^{31}P\text{-}\{^1H\}$ NMR spectrum showed a signal at δ 40.5, the chemical shift being diagnostic for an $Au(PPh_3)$ group.[1a] This peak, however is significantly broadened due to the position of the phosphorus atom *trans* to the boron atom β to the carbons in the CCB*B*B face of the cage. Moreover, the α-boron atoms probably bond weakly to the Au atom, as they do in the anion of **5b**,[2b] and this may also contribute to the broadening. The $^{11}B\text{-}\{^1H\}$ NMR spectrum displayed the customary broad peaks in the range δ −11.3 to −37.9. The peaks observed in the ^1H and $^{13}C\text{-}\{^1H\}$ NMR spectra are in accord with the formulation of **5a**.

The first reaction of compound **5a** studied was that with *trans*-$[RhCl(CO)(PPh_3)_2]$. In thf, in the presence of $TlBF_4$ to remove chloride as insoluble TlCl, the product isolated was the previously prepared species $[RhAu(CO)(PPh_3)_2(\eta^5\text{-}7,8\text{-}C_2B_9H_9Me_2)]$ **1b**, referred to above. A significant feature of the reaction is the transfer of the carbaborane cage from the gold to the rhodium. Compound **1b** displays a single CO stretch at 1983 cm^{-1} in its IR spectrum,[1b] and this was confirmed in the present study. However, the previously reported NMR data were

* *Supplementary data available:* see Instructions for Authors, *J. Chem. Soc., Dalton Trans.*, 1993, Issue 1, pp. xxiii–xxviii.

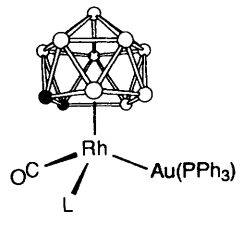

	L	
1a	PPh_3	CH
1b	PPh_3	CMe
1c	CO	CMe

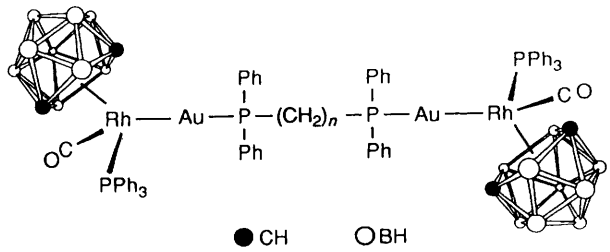

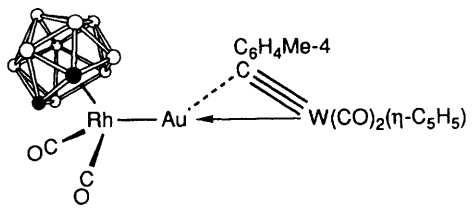

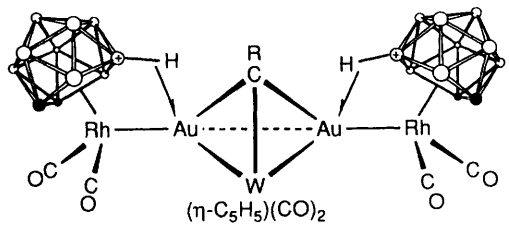

Table 1 Analytical[a] and physical data for the complexes

Compound	Colour	Yield (%)	Analysis (%) C	H
5a $[NEt_4][10\text{-}endo\text{-}\{Au(PPh_3)\}\text{-}nido\text{-}7,8\text{-}C_2B_9H_9Me_2]$	Yellow	65	[b] 48.4 (48.1)	6.7 (6.7)
6a $[exo\text{-}5,10\text{-}\{Rh(PPh_3)_2\}\text{-}5,10\text{-}(\mu\text{-}H)_2\text{-}10\text{-}endo\text{-}\{Au(PPh_3)\}\text{-}nido\text{-}7,8\text{-}C_2B_9H_7Me_2]$[c]	Red	70[d]	[e] 53.1 (53.2)	4.8 (4.7)
8b $[RhAu(PPh_3)_3(\eta^5\text{-}7,8\text{-}C_2B_9H_{11})]$	Orange	57	54.9 (55.2)	4.7 (4.6)
9 $[RhAu_2(\mu\text{-}H)(PPh_3)_3(\eta^5\text{-}7,8\text{-}C_2B_9H_9Me_2)]$	Bright yellow	26	48.4 (48.3)	4.3 (4.3)

[a] Calculated values are given in parentheses. [b] N, 1.9(1.9)%. [c] Exists in solution in equilibrium with its isomer **6b**, see text. [d] Yield is *ca.* 40% when prepared from $[Rh(cod)(PPh_3)_2][PF_6]$. [e] Crystallises with one molecule of CH_2Cl_2.

Table 2 Hydrogen-1 and carbon-13 NMR data[a] for the complexes

Compound	^1H (δ)[b]	^{13}C (δ)[c]
1b	1.47, 2.12 (s × 2, CMe), 7.14–7.73 (m, 30 H, Ph)	189.4 [d of d, CO, *J*(RhC) 66, *J*(PC) 20], 134.7–128.4 (Ph), 67.6 [d, *C*Me, *J*(PC) 25], 64.3 (br, *C*Me), 32.2, 26.6 (s × 2, C*Me*)
5a	1.20 (s, 6 H, CMe), 1.25 [t, br, 12 H, CH_2Me, *J*(HH) 6], 3.17 [q, 8 H, NCH_2, *J*(HH) 6], 7.48–7.73 (m, 15 H, Ph)	134.6 [d, C^2(Ph), *J*(PC) 14], 132.6 [d, C^1(Ph), *J*(PC) 50], 131.2 [C^4(Ph)], 129.2 [d, C^3(Ph), *J*(PC) 11], 54.7 (br, *C*Me), 53.4 (NCH_2), 22.7 (*CMe*), 7.9 (CH_2Me)
6a, 6b[d]	−5.4 (br, 2 H, BHRh), 1.18 (s, 6 H, CMe), 1.27* (s, 6 H, CMe), 7.32–7.50 (m, 45 H, Ph)	[e] 136.2 [AXX′, C^1(RhPPh), *J*(PP′) 31, *J*(PC) 61, *J*(P′C) 13], 134.6 [d, C^2(AuPPh), *J*(PC) 14], [f] 134.6 [AXX′, C^2(RhPPh), *N* 11], 131.5 [C^4(AuPPh)], 131.3 [d, C^1(AuPPh), *J*(PC) 54], 129.7 [C^4(RhPPh)], 129.3 [d, C^3(AuPPh), *J*(PC) 12], [f] 128.0 [AXX′, C^3(RhPPh), *N* 9], [g] 58.0 (*C*Me), 23.1* (*CMe*), 22.0 (*CMe*)
8b	2.25 (s, br, 2 H, CH), 6.93–7.56 (m, 45 H, Ph)	[f] 136.7 [AXX′, C^1(RhPPh), *N* 42], [f] 134.6 [AXX′, C^2(RhPPh), *N* 11], 134.4 [d, C^2(AuPPh), *J*(PC) 15], 131.9 [d, C^1(AuPPh), *J*(PC) 49], 131.5 [C^4(AuPPh)], 129.5 [d, C^3(AuPPh), *J*(PC) 10], 129.4 [C^4(RhPPh)], [f] 127.8 [AXX′, C^3(RhPPh), *N* 9], 42.9 (CH)
9	−3.92 [d of d of t, br, 1 H, μ-H, *J*(RhH) 20, *J*(PH) 28 and 26], 1.78 (br, 6 H, CMe), 7.11–7.91 (m, 45 H, Ph)	[h] 134.4–127.6 (Ph), 36.1, 27.0 (s × 2, *CMe*)

[a] Chemical shifts δ in ppm, coupling constants (*J*) in Hz, measurements in CD_2Cl_2 at room temperature unless otherwise stated. [b] Proton resonances for terminal BH groups occur as broad unresolved signals in the range δ *ca.* −2 to +3. [c] Hydrogen-1 decoupled, chemical shifts are positive to high frequency of $SiMe_4$. Measurements in CD_2Cl_2–CH_2Cl_2. [d] Peaks asterisked are due to isomer **6b**. [e] Weak resonances due to Ph carbons in compound **6b** occur in the range δ *ca.* 136–128. [f] Insufficient resolution prevents full analysis of coupling constants; $N = |J(AX) + J(AX')|$. [g] *C*Me nuclei in compound **6b** not observed. [h] Measured at −40 °C; compound is fluxional at ambient temperatures resulting in non-observation of signals due to the *C*Me nuclei under these conditions, while low solubility prevented observation of weak signals due to *C*Me nuclei at reduced temperatures.

unsatisfactory due to the relative insolubility of the complex, and, moreover, in the $^{31}P\text{-}\{^1H\}$ NMR spectrum the signal for the $Au(PPh_3)$ group was incorrectly measured. Consequently, the ^1H, $^{13}C\text{-}\{^1H\}$, and $^{31}P\text{-}\{^1H\}$ NMR spectra have been re-recorded on stronger solutions, and the $^{11}B\text{-}\{^1H\}$ spectrum also measured (Tables 2 and 3). The new data are in accord with the

Table 3 Boron-11 and phosphorus-31 NMR data[a] for the complexes

Compound	^{11}B (δ)[b]	^{31}P (δ)[c]
1b	−5.0 (br, 1 B), −7.5 (br, 1 B), −9.0 (br, 1 B), −12.9 (br, 4 B), −15.5 (br, 1 B), −17.6 (br, 1 B)	43.9 [d, PRh, *J*(RhP) 149], 36.3 [d, PAu, *J*(RhP) 8]
5a	−11.3 (br, 1 B), −18.1 (br, 2 B), −19.8 (br, 4 B), −26.3 (br, 1 B), −37.9 (br, 1 B)	40.5 (m, br)
6a, 6b	[d] −12.4 (br, 3 B), −18.6 (br, 2 B), −20.5 (br, 2 B), −30.0 (br, 1 B), −38.5 (br, 1 B)	[e] 46.9 [d, PRh, *J*(RhP) 184], 43.3 (m, vbr, PAu), 42.1* [d, PAu, *J*(RhP) 20], 37.3* [d, PRh, *J*(RhP) 133]
8b	−2.4 (br, 1 B), −6.8 (br, 1 B), −12.9 (br, 4 B), −22.5 (br, 2 B), −25.6 (br, 1 B)	39.0 [d of d, PRh, *J*(RhP) 142, *J*(PP) 6], 31.1 [d of t, PAu, *J*(RhP) 12, *J*(PP) 6]
9	−4.1 (br, 1 B), −8.2 (br, 1 B), −10.4 (br, 3 B), −13.4 (br, 2 B), −18.3 (br, 2 B)	[f] 46.1 [d of d of d, PRh, *J*(RhP) 140, *J*(PP) 14 and 10], 39.5 [d of d of d, PAu, *J*(RhP) 20, *J*(PP) 14 and 7], 29.5 [d of d of d, PAu, *J*(RhP) 17, *J*(PP) 10 and 7]

[a] Chemical shifts δ in ppm, coupling constants in Hz, measurements at room temperature in CD_2Cl_2 unless otherwise stated. [b] Hydrogen-1 decoupled, chemical shifts are positive to high frequency of $BF_3{\cdot}Et_2O$ (external). [c] Hydrogen-1 decoupled, chemical shifts are positive to high frequency of 85% H_3PO_4 (external). [d] Broad signals in the range δ 5.3 to −20.0 observed for compound **6b**; some peaks for **6b** are screened by peaks due to **6a**. [e] Peaks marked with an asterisk are due to compound **6b**. [f] Measured at −60 °C.

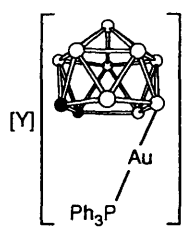

○ BH

	Y	●
5a	NEt_4	CMe
5b	$NMe_3(CH_2Ph)$	CH
5c	NEt_4	CH

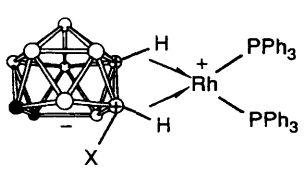

○ BH ⊕ B

	●	X
6a	CMe	$Au(PPh_3)$
7a	CMe	H
8a	CH	$Au(PPh_3)$

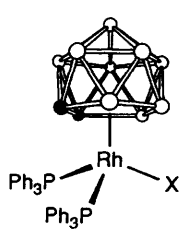

○ BH

	●	X
6b	CMe	$Au(PPh_3)$
7b	CMe	H
8b	CH	$Au(PPh_3)$

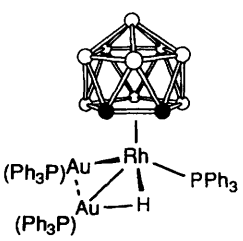

9 ● CMe ○ BH

formulation of **1b**, and are similar to those of other complexes of this type.

In a related synthesis to that which gave **1b**, treatment of $[Rh_2(\mu\text{-}Cl)_2(CO)_4]$ with **5a** in the presence of $TlBF_4$ gave complex **1c**, previously prepared from the reaction between $[AuCl(PPh_3)]$ and $[NEt_4][Rh(CO)_2(\eta^5\text{-}7,8\text{-}C_2B_9H_9Me_2)]$.[1a] Again, the new synthesis of **1c** involves transfer of the carbaborane cage from the gold in **5a** to the rhodium centre in the product. Compound **1c** was identified by its IR [ν_{max}(CO) 2048vs and 1996s cm^{-1}] and ^1H NMR spectra.

The reaction between compound **5a** and $[RhCl(PPh_3)_3]$ in the presence of $TlBF_4$ was next investigated. Examination of the NMR data (^1H, $^{13}C\text{-}\{^1H\}$, $^{11}B\text{-}\{^1H\}$ and $^{31}P\text{-}\{^1H\}$) revealed that the product **6** existed in solution as a mixture of two isomers **6a** and **6b**, formed in a ratio of *ca.* 6:1 based on relative peak intensities in the $^{31}P\text{-}\{^1H\}$ NMR spectrum. Crystals of the major isomer were grown from CH_2Cl_2–hexane, and an X-ray diffraction study (Table 4 and Fig. 1) revealed that the molecule was [*exo*-5,10-{$Rh(PPh_3)_2$}-5,10-(μ-H)$_2$-10-*endo*-{$Au(PPh_3)$}-*nido*-7,8-$C_2B_9H_7Me_2$] **6a**.

In the crystal structure of compound **6a** a $Rh(PPh_3)_2$ fragment is attached to the 7,8-$C_2B_9H_9Me_2$ cage *via* two B–H→Rh three-centre two-electron bonds, employing boron atoms B(4) and B(9). The atom B(4) is in the open pentagonal C_2B_3 ring of the *nido*-C_2B_9 fragment and in the β site with respect to the carbons, while B(9) lies in the B_5 pentagonal ring above B(4). The μ-H atoms [H(4) and H(9)] were located in the final electron-density difference map. The $Au(PPh_3)$ fragment is attached to the open C_2B_3 face of the cage, with connectivities to B(3), B(4) and B(5) of 2.48(2), 2.22(2) and 2.60(3) Å, respectively. It is noteworthy that the Au–B(4) separation of 2.22(2) Å is the shortest of the three and may be compared with that found [2.222(9) Å] for the corresponding Au–B distance in the anion of **5b** studied by Hamilton and Welch.[2b] Although the *endo*-$Au(PPh_3)$ unit in **6a** is more tightly bound to B(4) than B(3) or B(5), it is displaced towards B(3). A similar feature is observed in the structure of **5b**. In the latter, the angle P–Au–B_β is 169.3(2)°, to be compared with 172.1(7)° for P(1)–Au–B(4) in **6a**.

The structure established for **6a** bears a striking resemblance to those found for a family of *exo*-phosphinerhoda-*nido*-carbaboranes [*exo*-5,10-{$Rh(PPh_3)_2$}-5,10-(μ-H)$_2$-10-*endo*-H-7,8-*nido*-$C_2B_9H_7R_2$] (R = alkyl or aryl) studied by Hawthorne and co-workers.[6] These species may be viewed as ion pairs in which a cationic $[Rh(PPh_3)_2]^+$ fragment is tightly held to a $[nido\text{-}7,8\text{-}C_2B_9H_{10}R_2]^-$ anion through a pair of *cis*-B–H→Rh bonds. Similarly, **6a** may be regarded as a zwitterionic complex formed from an *exo*-$[Rh(PPh_3)_2]^+$ cation and the anion of **5a**. The $Au(PPh_3)$ unit in **6a** formally replaces the 10-*endo*-H atom in Hawthorne's complexes, *e.g.* **7a**, a species which exists in solution in equilibrium with a minor isomer **7b**.[6]

As mentioned above, in solution compound **6a** exists in equilibrium with a minor isomer **6b**, as evidenced by

Table 4 Selected internuclear distances (Å) and angles (°) for the complex [*exo*-5,10-{Rh(PPh$_3$)$_2$}-5,10-(μ-H)$_2$-10-*endo*-{Au(PPh$_3$)}-*nido*-7,8-$C_2B_9H_7Me_2$]·CH_2Cl_2 **6a**

Au–P(1)	2.262(6)	Au–B(3)	2.48(2)	Au–B(4)	2.22(2)	Au–B(5)	2.60(3)
Rh–P(2)	2.214(6)	Rh–P(3)	2.241(4)	Rh–B(4)	2.41(2)	Rh–B(9)	2.37(2)
Rh–H(4)	1.7[a]	Rh–H(9)	1.6[a]	C(1)–C(2)	1.56(3)	C(1)–B(5)	1.58(3)
C(1)–B(6)	1.76(3)	C(1)–B(10)	1.75(3)	C(1)–C(10)	1.51(3)	C(2)–B(3)	1.63(4)
C(2)–B(6)	1.69(4)	C(2)–B(7)	1.70(3)	C(2)–C(20)	1.50(2)	B(3)–B(4)	1.82(2)
B(3)–B(7)	1.85(4)	B(3)–B(8)	1.78(3)	B(4)–B(5)	1.81(4)	B(4)–B(8)	1.75(3)
B(4)–B(9)	1.70(4)	B(4)–H(4)	1.1[a]	B(5)–B(9)	1.78(3)	B(5)–B(10)	1.78(4)
B(6)–B(7)	1.71(4)	B(6)–B(10)	1.77(3)	B(6)–B(11)	1.80(3)	B(7)–B(8)	1.78(3)
B(7)–B(11)	1.78(3)	B(8)–B(9)	1.81(3)	B(8)–B(11)	1.80(4)	B(9)–B(10)	1.69(4)
B(9)–B(11)	1.75(3)	B(9)–H(9)	1.2[a]	B(10)–B(11)	1.78(3)		

P(1)–Au–B(3)	138.8(4)	P(1)–Au–B(4)	172.1(7)	B(3)–Au–B(4)	45.2(6)
P(1)–Au–B(5)	141.5(5)	B(3)–Au–B(5)	67.7(7)	B(4)–Au–B(5)	43.2(8)
P(2)–Rh–P(3)	95.8(2)	P(2)–Rh–B(4)	111.8(7)	P(3)–Rh–B(4)	152.4(7)
P(2)–Rh–B(9)	153.0(5)	P(3)–Rh–B(9)	110.8(5)	B(4)–Rh–B(9)	41.8(8)
P(2)–Rh–H(4)	88[a]	P(3)–Rh–H(4)	174[a]	B(4)–Rh–H(4)	24[a]
B(9)–Rh–H(4)	66[a]	P(2)–Rh–H(9)	166[a]	P(3)–Rh–H(9)	88[a]
B(4)–Rh–H(9)	65[a]	B(9)–Rh–H(9)	29[a]	H(4)–Rh–H(9)	87[a]
Au–B(3)–C(2)	91.9(10)	Au–B(3)–B(4)	59.6(9)	Au–B(3)–B(7)	143.8(13)
Au–B(3)–B(8)	117.8(10)	Au–B(3)–H(3)	90[b]	Au–B(4)–Rh	132.2(11)
Au–B(4)–B(3)	75.2(10)	Rh–B(4)–B(3)	143.2(13)	Au–B(4)–B(5)	79.9(11)
Rh–B(4)–B(5)	105.9(11)	Au–B(4)–B(8)	135.0(11)	Rh–B(4)–B(8)	88.7(11)
Au–B(4)–B(9)	140.5(16)	Rh–B(4)–B(9)	68.0(9)	Au–B(4)–H(4)	101[a]
Rh–B(4)–H(4)	38[a]	Au–B(5)–C(1)	90.4(12)	Au–B(5)–B(4)	56.9(11)
Au–B(5)–B(9)	113.5(14)	Au–B(5)–B(10)	143.2(11)	Au–B(5)–H(5)	95[b]
Rh–B(9)–B(4)	70.2(11)	Rh–B(9)–B(5)	108.3(14)	Rh–B(9)–B(8)	88.4(12)
Rh–B(9)–B(10)	160.7(12)	Rh–B(9)–B(11)	135.5(13)	Rh–B(9)–H(9)	37[a]
Rh–H(4)–B(4)	119[a]	Rh–H(9)–B(9)	114[a]		

[a] H(4) and H(9) in fixed positions. [b] H(3) and H(5) in calculated positions.

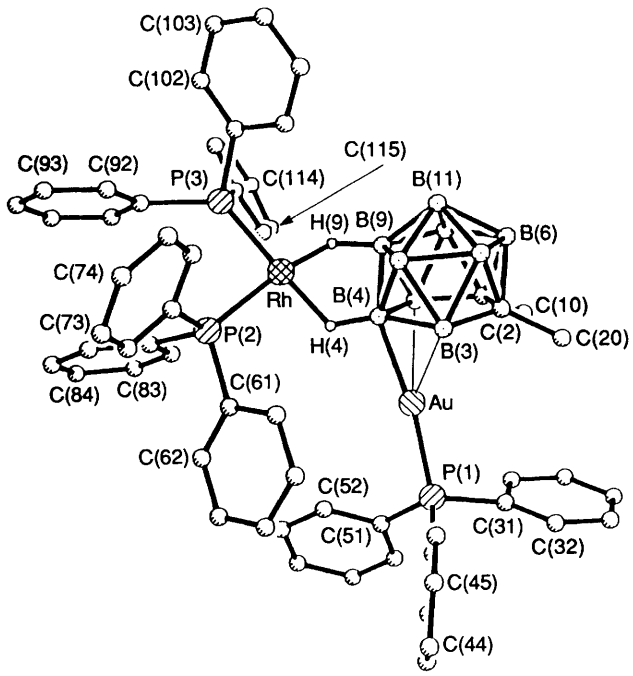

Fig. 1 Molecular structure of [*exo*-5,10-{Rh(PPh$_3$)$_2$}-5,10-(μ-H)$_2$-10-*endo*-{Au(PPh$_3$)}-*nido*-7,8-$C_2B_9H_7Me_2$] **6a**, showing the crystallographic labelling scheme

the appearance of extra but much weaker signals in the NMR spectra. As discussed below, **6b** is formulated as [RhAu(PPh$_3$)$_3$(η^5-7,8-$C_2B_9H_9Me_2$)] in which a *closo*-3,1,2-RhC_2B_9 cage system is present. This structure corresponds to a complete transfer of the 7,8-$C_2B_9H_9Me_2$ ligand from the gold to the rhodium, giving the latter an 18-electron configuration, as opposed to the 16-electron valence shell for rhodium in what may formally be viewed as the intermediate **6a**.

In the ^{1}H NMR spectrum of the species **6** (Table 2) a broad signal at δ −5.4 is attributable to the B–H→Rh hydrogens of **6a**. The observation of one signal suggests that the molecule is fluxional. In agreement, the ^{31}P-{^{1}H} NMR spectrum (Table 3) shows only one resonance for the Rh(PPh$_3$)$_2$ fragment, a doublet at δ 46.9 [*J*(RhP) 184 Hz]. The dynamic behaviour very probably involves rotation of the Rh(PPh$_3$)$_2$ group, together with other processes, as found with **7a** and other structurally similar *exo-nido* species.[6] Complexes of type **7a** also show only one doublet resonance with *J*(RhP) 185 Hz. A very broad multiplet in the ^{31}P-{^{1}H} NMR spectrum of **6a** is attributable to the Au(PPh$_3$) group.

Isomer **6b** displays a resonance in its ^{31}P-{^{1}H} NMR spectrum at δ 37.3 [*J*(RhP) 133 Hz], similar to that of species such as **7b**. In the ^{1}H NMR spectrum of the isomeric mixture **6**, peaks for the cage CMe groups are seen at δ 1.18 (**6a**) and 1.27 (**6b**). In the ^{13}C-{^{1}H} NMR spectrum, resonances for the C*Me* groups occur at δ 22.0 (**6a**) and 23.1 (**6b**). However, the peak for the *C*Me nuclei is only observed for **6a** (δ 58.0), that for **6b** being too weak to be seen in the noise.

The existence of the isomeric pairs **6a** and **6b**, and **7a** and **7b**, is an interesting demonstration of the isolobal model, with Au(PPh$_3$) groups in the species **6** replacing hydrogen atoms in **7**.[3,7] As mentioned, isomer **6a** is favoured with respect to **6b**. With species of type **7** the *exo-nido* isomer is also the dominant isomer in solution and indeed the only isomer detected in some cases.[6]

Whereas the reaction between compound **5a** and [RhCl(PPh$_3$)$_3$] afforded the species **6**, that with [Rh(cod)(PPh$_3$)$_2$][PF$_6$] (cod = cycloocta-1,5-diene) in CH_2Cl_2 in the presence of molecular hydrogen gave a mixture of **6** and the rhodium–digold compound [RhAu$_2$(μ-H)(PPh$_3$)$_3$(η^5-7,8-$C_2B_9H_9Me_2$)] **9**. Addition of hydrogen to the mixture of **5a** and [Rh(cod)(PPh$_3$)$_2$][PF$_6$] was done to facilitate displacement of the cod ligand.[8] The nature of the product **9** was not determined until after an X-ray diffraction study. The results of the latter are summarised in Table 5, and the structure is shown in Fig. 2.

The core of the molecule is a RhAu$_2$ unit [Au(1)–Rh 2.695(2),

Table 5 Selected internuclear distances (Å) and angles (°) for the complex $[RhAu_2(\mu\text{-}H)(PPh_3)_3(\eta^5\text{-}7,8\text{-}C_2B_9H_9Me_2)]\cdot 2CH_2Cl_2$ **9**

Au(1)···Au(2)	2.905(2)	Au(1)–Rh	2.695(2)	Au(1)–P(1)	2.270(7)	Au(1)–H(001)	1.82*
Au(2)–Rh	2.601(3)	Au(2)–P(2)	2.269(8)	Rh–P(3)	2.279(8)	Rh–C(1)	2.35(3)
Rh–C(2)	2.28(3)	Rh–B(3)	2.23(3)	Rh–B(4)	2.29(3)	Rh–B(5)	2.22(3)
Rh–H(001)	1.79*	C(1)–C(2)	1.69(3)	C(1)–C(10)	1.57(3)	C(1)–B(5)	1.72(5)
C(1)–B(6)	1.72(4)	C(1)–B(10)	1.67(3)	C(2)–C(20)	1.53(3)	C(2)–B(3)	1.78(4)
C(2)–B(6)	1.79(4)	C(2)–B(7)	1.71(3)	B(3)–B(4)	1.81(5)	B(3)–B(7)	1.82(5)
B(3)–B(8)	1.76(4)	B(4)–B(5)	1.91(4)	B(4)–B(8)	1.79(5)	B(4)–B(9)	1.83(4)
B(5)–B(9)	1.80(4)	B(5)–B(10)	1.82(5)				

Au(2)–Au(1)–Rh	55.2(1)	Au(2)–Au(1)–P(1)	124.1(2)	Rh–Au(1)–P(1)	163.7(2)
Au(2)–Au(1)–H(001)	92*	Rh–Au(1)–H(001)	41*	H(001)–Au(1)–P(1)	144*
Au(1)–Au(2)–Rh	58.3(1)	Au(1)–Au(2)–P(2)	128.2(2)	Rh–Au(2)–P(2)	173.0(2)
Au(1)–Rh–Au(2)	66.5(1)	Au(1)–Rh–P(3)	99.4(2)	Au(2)–Rh–P(3)	85.2(2)
Au(1)–Rh–C(1)	127.0(7)	Au(2)–Rh–C(1)	147.4(5)	P(3)–Rh–C(1)	116.7(6)
Au(1)–Rh–C(2)	91.3(5)	Au(2)–Rh–C(2)	117.5(5)	P(3)–Rh–C(2)	157.3(6)
C(1)–Rh–C(2)	43.0(8)	Au(1)–Rh–B(3)	88.2(7)	Au(2)–Rh–B(3)	74.0(8)
P(3)–Rh–B(3)	152.9(9)	Au(1)–Rh–B(4)	124.9(7)	Au(2)–Rh–B(4)	70.4(8)
P(3)–Rh–B(4)	110(1)	Au(1)–Rh–B(5)	167(1)	Au(2)–Rh–B(5)	115.9(9)
P(3)–Rh–B(5)	93(1)	Au(1)–Rh–H(001)	42*	Au(2)–Rh–H(001)	104*
H(001)–Rh–P(3)	84*	H(001)–Rh–C(1)	103*	H(001)–Rh–C(2)	91*
H(001)–Rh–B(3)	117*	H(001)–Rh–B(4)	164*	H(001)–Rh–B(5)	139*
Au(1)–H(001)–Rh	97*				

* H(001) in calculated position.

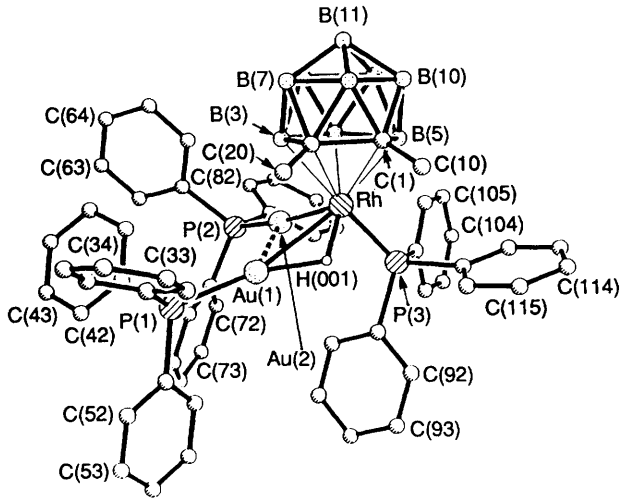

Fig. 2 Molecular structure of $[RhAu_2(\mu\text{-}H)(PPh_3)_3(\eta^5\text{-}7,8\text{-}C_2B_9H_9Me_2)]$ **9**, showing the crystallographic labelling scheme

Au(2)–Rh 2.601(3), Au(1)···Au(2) 2.905(2) Å]. The gold and rhodium atoms each carry a PPh_3 ligand and the rhodium is also co-ordinated by the *nido*-7,8-$C_2B_9H_9Me_2$ cage fragment in the usual pentahapto manner. The Au–Rh bond lengths in **9** are comparable with those found in **4** [2.715(2) Å] and in $[WRhAu(\mu\text{-}CC_6H_4Me\text{-}4)(CO)_3(PPh_3)(\eta\text{-}C_5H_5)(\eta^5\text{-}7,8\text{-}C_2B_9H_{11})]$ [2.640(1) Å], a molecule similar to **3** but with a 7,8-$C_2B_9H_{11}$ cage.[1a] The Au···Au separation in **9** [2.905(2) Å] compares with that in **4** [2.969(2) Å], and these distances initially suggest that there is little direct gold–gold bonding in either molecule. However, a review by Hall and Mingos[9] indicates that this might not be the case and that there may be a significant electronic interaction between gold atoms with separations of this order.

A feature of major interest in the structure of compound **9** is the presence of the hydride ligand spanning the Rh–Au(1) bond. Although not located in the electron-density difference maps, H(001) is assigned to the site suggested by potential-energy minimisation calculations.[10] The justification for this calculated location of H(001) arises from the appreciable distortion of the Rh–Au(1)–P(1) group [163.7(2)°] from a linear unit, in comparison with the Rh–Au(2)–P(2) group [173.0(2)°]. Moreover, the ^1H NMR spectrum of **9** clearly revealed the presence of the hydride with a resonance at δ −3.92 (Table 2). The origin of this hydride must be the molecular hydrogen introduced into the reaction mixture. It has been established[8] that treatment of complexes of the type $[Rh(diene)(PPh_3)_2]^+$ with molecular hydrogen removes the diene ligand, which is subsequently hydrogenated, to give a rhodium hydride complex $[RhH_2(solv)_2(PPh_3)_2]^+$ (solv = solvent). Such a complex probably lies on the path to the formation of **9**. The structure of **9** is a further example of transfer of the carbaborane cage in **5a** to an η^5-bonding mode at the rhodium centre.

The molecule **9** is fluxional, but its poor solubility inhibited measurement of limiting low-temperature spectra. In the ^1H NMR spectrum, measured at room temperature, the aforementioned μ-H resonance at δ −3.92 appears as a doublet of doublet of triplets, but the signal is broadened slightly. On cooling to −60 °C only a broad multiplet is observed. In a ^1H-$\{^{31}P\}$ NMR spectrum the multiplet became a doublet [J(RhH) 20 Hz], but selective ^{31}P decoupling experiments were unsuccessful. Whereas in the ^1H NMR spectrum at room temperature only one broad resonance for the cage CMe groups is seen (δ 1.78), at −60 °C the signal was resolved into two peaks at δ 1.29 and 2.05. In the ^{13}C-$\{^1H\}$ NMR spectrum at room temperature the *CMe* peaks are not seen, but they are observed at δ 36.1 and 27.0 at −40 °C. Non-observation of the *C*Me nuclei is due to the weak spectrum, resulting from the low solubility of the complex.

The room-temperature ^{31}P-$\{^1H\}$ NMR spectrum of compound **9** showed a doublet of triplets (δ 45.1) for the $Rh(PPh_3)$ group, and a very broad band centred at *ca.* δ 35 for the $Au(PPh_3)$ fragments. Data from a spectrum measured at −60 °C are listed in Table 3, and were rationalised with an NMR simulation program.

A proposed mechanism for the dynamic behaviour, based on the NMR data and the X-ray analysis, is shown in Scheme 1. The fluxional process is an interconversion between two enantiomers, which chiefly involves exchange of the μ-H atom from one Rh–Au bond to the other, accompanied by a partial rotation of the cage. The process is occurring on the NMR time-scale at room temperature, as indicated by the broadness of the CMe resonances in the ^1H NMR spectrum and the extremely broad signal for the $Au(PPh_3)$ groups in the ^{31}P-$\{^1H\}$ NMR spectrum. It is suggested that the transition state involves a triply bridging hydride ligand, with the intermediate having a mirror plane, a situation implied by the cage CMe groups

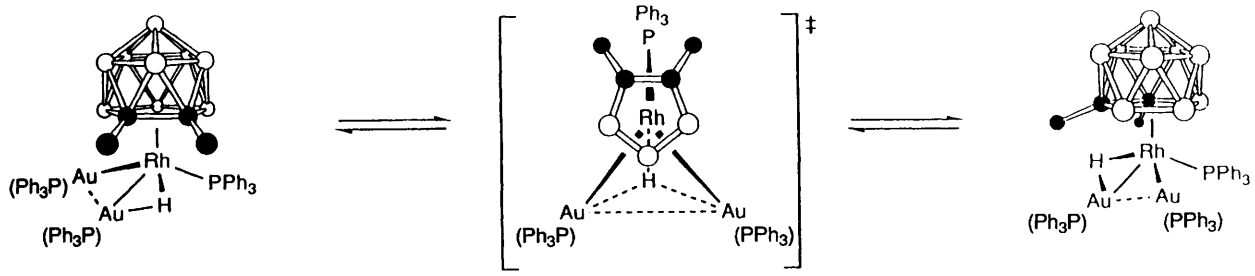

Scheme 1 Proposed mechanism for the dynamic behaviour of compound **9** (complete cage not shown in transition state)

becoming equivalent at higher temperatures. Reduction of the temperature to below −40 °C slows down this interconversion sufficiently to freeze out the 'static' enantiomers, which may be equated with the crystal structure of **9** previously described. Thus two signals are observed for the C*Me* groups in the ^{1}H and ^{13}C-{^{1}H} NMR spectra.

Finally, the reaction between compound **5c** and [RhCl(PPh$_3$)$_3$] was investigated. The salt **5c** contains a 7,8-$C_2B_9H_{11}$ cage instead of the 7,8-$C_2B_9H_9Me_2$ ligand. Previous studies[1,11] have shown that the reactivity pattern displayed by reagents containing these *nido*-icosahedral fragments depends critically on whether the cages have CMe or CH vertices. This difference is again seen in the present work. The reaction afforded [RhAu(PPh$_3$)$_3$(η^5-7,8-$C_2B_9H_{11}$)] **8b**, there being no evidence for an *exo-nido* isomer **8a** similar to **6a**. We have noted previously that the presence of CMe groups in the C_2B_9 framework activates BH vertices to form B–H→M bonds. Data fully characterising **8b**, which is structurally similar to **1a** but with a PPh$_3$ group replacing a CO group, are given in Tables 1–3.

The results described in this paper indicate that the salts **5** are potentially useful reagents for preparing mixed-metal complexes containing gold, and further studies are in progress. The observed transfer of the *nido*-7,8-$C_2B_9H_9R_2$ (R = Me or H) groups from gold to rhodium in the reactions is, with hindsight, perhaps to be expected, in view of the isolobal mapping of the reagents **5** with salts of the anions [10-*endo*-H-*nido*-7,8-$C_2B_9H_9R_2$]$^-$. Nevertheless, the equilibrium in solution between **6a** and **6b**, and between **7a** and **7b**,[6] is a striking illustration of how Au(PPh$_3$) groups may replace H atoms in cluster chemistry.

Experimental

All experiments were carried out under a dry, oxygen-free nitrogen atmosphere using standing Schlenk-tube techniques. Solvents were dried and distilled under a nitrogen atmosphere before use. The reagents [NHMe$_3$][7,8-$C_2B_9H_{10}Me_2$],[12] [AuCl(PPh$_3$)],[13] trans-[RhCl(CO)(PPh$_3$)$_2$],[14] [RhCl(PPh$_3$)$_3$],[15] [Rh$_2$(μ-Cl)$_2$(CO)$_4$],[16] and [Rh(cod)(PPh$_3$)$_2$][PF$_6$][8] were made by procedures previously described. The salt [NEt$_4$][10-*endo*-{Au(PPh$_3$)}-*nido*-7,8-$C_2B_9H_{11}$] **5c** was prepared by the method used to obtain **5b**.[2b] Sodium hydride, supplied as a 60% dispersion in oil by Aldrich, was weighed out, washed with two portions of hexane (2 × *ca.* 10 cm^3) and dried *in vacuo* immediately prior to use. Light petroleum refers to that fraction of b.p. 40–60 °C. Chromatography columns were packed with alumina (Aldrich, Brockmann Activity II). Celite pads used for filtration were *ca.* 3 cm thick. Analytical and other data for the new compounds are given in Tables 1–3. The NMR measurements were made with JEOL GX270 and GX400 instruments, IR measurements with a Perkin-Elmer 1600 series FT IR instrument.

Synthesis of the Salt [NEt$_4$][10-*endo*-{Au(PPh$_3$)}-*nido*-7,8-$C_2B_9H_9Me_2$].—A thf (25 cm^3) solution of [NHMe$_3$][7,8-$C_2B_9H_{10}Me_2$] (0.09 g, 0.41 mmol) in a round-bottom flask (250 cm^3) was treated with a NaH (0.08 g, 2.0 mmol) suspension in thf (25 cm^3). This mixture was refluxed under nitrogen for *ca.* 12 h. Taking care not to take up any excess of NaH that had settled to the bottom of the flask, the freshly formed solution of Na$_2$[7,8-$C_2B_9H_9Me_2$] obtained was combined with a thf (15 cm^3) solution of [AuCl(PPh$_3$)] (0.20 g, 0.27 mmol) and the mixture was stirred at room temperature for *ca.* 7 h. The volume of solvent was reduced *in vacuo* to *ca.* 25 cm^3 and [NEt$_4$]Cl (0.08 g, 0.44 mmol) was added. After *ca.* 15–30 min sudden precipitation of NaCl occurred. Solvent was removed *in vacuo*, the residue was taken up in CH_2Cl_2 (30 cm^3) and filtered through a Celite pad. After removing solvent *in vacuo*, the product was crystallised from CH_2Cl_2–hexane (10 cm^3, 1:4) to give yellow *microcrystals* of [NEt$_4$][10-*endo*-{Au(PPh$_3$)}-*nido*-7,8-$C_2B_9H_9Me_2$] **5a** (0.19 g).

Synthesis of the Complexes [RhAu(CO)(PPh$_3$)L(η^5-7,8-$C_2B_9H_9Me_2$)].—(*i*) The compounds **5a** (0.10 g, 0.13 mmol), *trans*-[RhCl(CO)(PPh$_3$)$_2$] (0.09 g, 0.13 mmol) and TlBF$_4$ (0.05 g, 0.17 mmol) were stirred together in thf (30 cm^3) at room temperature for *ca.* 12 h, after which time there was no further change in the IR spectrum of the mixture. Solvent was removed *in vacuo*, CH_2Cl_2 (30 cm^3) added to the residue and the suspension filtered through a Celite pad. Solvent was reduced to *ca.* 4 cm^3 *in vacuo*, and the solution was then chromatographed. Elution with CH_2Cl_2–light petroleum, initially 2:3 and finally 1:1, removed a broad yellow fraction. Solvent was removed *in vacuo* and the solid crystallised from CH_2Cl_2–light petroleum (10 cm^3, 1:3) to give bright yellow *microcrystals* of [RhAu(CO)(PPh$_3$)$_2$(η^5-7,8-$C_2B_9H_9Me_2$)] **1b** (0.11 g, 85%).

(*ii*) In a similar manner, compounds **5a** (0.13 g, 0.17 mmol), [Rh$_2$(μ-Cl)$_2$(CO)$_4$] (0.03 g, 0.09 mmol) and TlBF$_4$ (0.06 g, 0.22 mmol) afforded yellow *microcrystals* of [RhAu(CO)$_2$(PPh$_3$)(η^5-7,8-$C_2B_9H_9Me_2$)] **1c** (0.07 g, 53%) after chromatography at −30 °C, and crystallisation from CH_2Cl_2–hexane (10 cm^3, 1:4).

Reactions of [NEt$_4$][10-*endo*-{Au(PPh$_3$)}-*nido*-7,8-$C_2B_9H_9Me_2$] *with* [RhCl(PPh$_3$)$_3$] *and with* [Rh(cod)(PPh$_3$)$_2$][PF$_6$].—(*i*) A mixture of compound **5a** (0.20 g, 0.27 mmol), [RhCl(PPh$_3$)$_3$] (0.25 g, 0.27 mmol) and TlBF$_4$ (0.09 g, 0.32 mmol) was dissolved in thf (25 cm^3) and stirred at room temperature for *ca.* 20 h. Solvent was removed *in vacuo*, the residue was treated with CH_2Cl_2 (30 cm^3) and the suspension filtered through a Celite pad. Solvent was then reduced *in vacuo* to *ca.* 3 cm^3 and the solution chromatographed at −30 °C. Elution with CH_2Cl_2–hexane (1:1) removed a broad red band. Solvent was removed *in vacuo* from the eluate and the solid was crystallised from CH_2Cl_2–hexane (10 cm^3, 1:4) to afford red *microcrystals* of [*exo*-5,10-{Rh(PPh$_3$)$_2$}-5,10-(μ-H)$_2$-10-*endo*-{Au(PPh$_3$)}-*nido*-7,8-$C_2B_9H_7Me_2$] **6a** (0.23 g).

(*ii*) The compounds **5a** (0.20 g, 0.27 mmol) and [Rh(cod)(PPh$_3$)$_2$][PF$_6$] (0.24 g, 0.27 mmol) were dissolved in CH_2Cl_2 (50 cm^3) in a jacketed Schlenk tube and the solution cooled to −20 °C. Hydrogen was bubbled through at a fairly rapid rate (*ca.* 2 bubbles s^{-1}). After 3 h the solution was warmed to room temperature, while maintaining the hydrogen stream. Once ambient temperature was obtained and the flow of

Table 6 Crystallographic data[a]

Compound	**6a**	**9**
Crystal dimensions (mm)	0.10 × 0.15 × 0.30	0.50 × 0.30 × 0.30
Molecular formula	$C_{58}H_{60}AuB_9P_3Rh\cdot CH_2Cl_2$	$C_{58}H_{61}Au_2B_9P_3Rh\cdot 2CH_2Cl_2$
M	1332.2	1615.0
Crystal colour, shape	Red prisms	Orange prisms
Crystal system	Triclinic	Monoclinic
Space group	$P\bar{1}$	$P2_1/c$
a/Å	12.575(5)	20.516(9)
b/Å	13.472(3)	14.373(7)
c/Å	19.975(5)	22.739(8)
α/°	84.89(2)	
β/°	77.34(3)	106.18(3)
γ/°	64.35(2)	
U/Å^3	2976(2)	6440(5)
Z	2	4
D_c/g cm^{-3}	1.49	1.67
μ(Mo-Kα)/cm^{-1}	29.4	50.8
F(000)	1328	3144
T/K	293	293
Data collection limits (2θ/°)	5–45	5–40
No. of reflections collected	8525	5187
No. of observed data used	3949	3262
Criterion for data (n) used [$F_o \geqslant n\sigma(F_o)$]	5	5
R (R')[b]	0.061 (0.056)	0.063 (0.066)
Final electron-density difference features (maximum, minimum)/e Å^{-3}	1.60, −0.85	1.74, −1.96

[a] Data collected on a Siemens R3m/V four-circle diffractometer operating in the Wyckoff ω-scan mode; graphite-monochromated Mo-Kα X-radiation, $\bar{\lambda}$ = 0.710 69 Å. Refinement was by full-matrix least squares with a weighting scheme of the form $w^{-1} = [\sigma^2(F_o) + g|F_o|^2]$ with g = 0.0006 (**6a**), 0.0013 (**9**); $\sigma^2(F_o)$ is the variance in F_o due to counting statistics; g was chosen so as to minimise variation in $\Sigma w(|F_o| - |F_c|)^2$ with $|F_o|$. [b] $R = \Sigma||F_o| - |F_c||/\Sigma|F_o|$, $R' = \Sigma w^{\frac{1}{2}}||F_o| - |F_c||/\Sigma w^{\frac{1}{2}}|F_o|$.

Table 7 Atomic positional parameters (fractional coordinates × 10^4) for compound **6a**, with estimated standard deviations (e.s.d.s) in parentheses

Atom	x	y	z	Atom	x	y	z
Au	1 852(1)	10 757(1)	1 817(1)	Rh	3 369(1)	7 765(1)	2 864(1)
P(1)	2 132(5)	12 141(4)	1 193(3)	P(2)	4 613(4)	8 204(3)	3 270(2)
P(3)	4 315(4)	5 949(3)	3 031(2)	C(1)	274(18)	9 644(14)	1 629(9)
C(2)	−456(17)	10 475(15)	2 239(10)	B(3)	350(19)	10 506(16)	2 769(10)
B(4)	1 806(18)	9 360(17)	2 477(12)	B(5)	1 635(21)	8 953(17)	1 683(11)
B(6)	−779(21)	9 373(18)	2 260(13)	B(7)	−722(21)	9 874(19)	3 001(12)
B(8)	764(20)	9 185(16)	3 163(10)	B(9)	1 579(17)	8 205(15)	2 461(10)
B(10)	647(23)	8 301(16)	1 937(12)	B(11)	98(20)	8 433(17)	2 840(11)
C(10)	−44(20)	9 950(18)	931(9)	C(20)	−1 447(17)	11 536(16)	2 085(11)
C(31)	1 066(14)	12 747(13)	624(7)	C(32)	15	13 715	782
C(33)	−829	14 069	360	C(34)	−621	13 454	−220
C(35)	430	12 485	−378	C(36)	1 273	12 132	44
C(41)	1 880(11)	13 314(8)	1 689(6)	C(42)	2 336	14 066	1 398
C(43)	2 189	14 940	1 789	C(44)	1 585	15 062	2 473
C(45)	1 129	14 311	2 765	C(46)	1 276	13 436	2 373
C(51)	3 633(9)	11 713(10)	702(7)	C(52)	4 534	10 996	1 041
C(53)	5 742	10 646	722	C(54)	6 050	11 013	65
C(55)	5 150	11 730	−274	C(56)	3 941	12 080	45
C(61)	4 461(11)	9 617(7)	3 113(6)	C(62)	5 406	9 886	2 797
C(63)	5 216	10 987	2 730	C(64)	4 080	11 819	2 980
C(65)	3 135	11 550	3 296	C(66)	3 325	10 449	3 362
C(71)	4 404(10)	8 212(9)	4 210(4)	C(72)	5 027	8 606	4 531
C(73)	4 784	8 685	5 245	C(74)	3 919	8 369	5 638
C(75)	3 296	7 976	5 317	C(76)	3 539	7 897	4 603
C(81)	6 190(8)	7 448(8)	2 905(6)	C(82)	6 435	7 308	2 195
C(83)	7 624	6 814	1 837	C(84)	8 569	6 460	2 188
C(85)	8 324	6 601	2 897	C(86)	7 135	7 095	3 256
C(91)	5 730(8)	5 250(8)	3 335(6)	C(92)	5 703	5 265	4 036
C(93)	6 768	4 740	4 283	C(94)	7 861	4 200	3 829
C(95)	7 888	4 185	3 128	C(96)	6 823	4 710	2 881
C(101)	3 340(9)	5 412(8)	3 638(5)	C(12)	3 770	4 313	3 843
C(103)	2 995	3 933	4 276	C(104)	1 790	4 651	4 505
C(105)	1 360	5 749	4 300	C(106)	2 135	6 129	3 866
C(111)	4 719(10)	5 205(9)	2 226(5)	C(112)	5 093	4 070	2 190
C(113)	5 471	3 549	1 552	C(114)	5 475	4 162	951
C(115)	5 102	5 296	988	C(116)	4 724	5 818	1 626
C(200)*	1 242(24)	1 003(20)	5 167(12)	Cl(1)*	1 944(7)	1 795(6)	5 242(4)
Cl(2)*	266(8)	1 465(7)	4 628(4)				

* Solvent molecule.

Table 8 Atomic positional parameters (fractional coordinates × 10^4) for compound **9**, with e.s.d.s in parentheses

Atom	*x*	*y*	*z*	Atom	*x*	*y*	*z*
Au(1)	1 566(1)	2 301(1)	8 849(1)	Au(2)	3 008(1)	2 121(1)	9 451(1)
Rh	2 189(1)	706(1)	9 314(1)	P(1)	991(4)	3 670(4)	8 723(3)
P(2)	3 809(4)	3 255(4)	9 665(3)	P(3)	2 626(4)	291(4)	8 534(3)
C(1)	1 742(14)	−496(15)	9 782(10)	C(2)	1 535(14)	582(15)	9 972(9)
C(10)	1 187(14)	−1 076(18)	9 307(11)	C(20)	817(13)	948(16)	9 684(10)
B(3)	2 277(17)	1 270(19)	10 248(12)	B(4)	3 011(18)	581(20)	10 226(13)
B(5)	2 601(19)	−550(20)	9 864(13)	B(6)	1 560(18)	−384(20)	10 472(13)
B(7)	1 859(19)	681(21)	10 750(13)	B(8)	2 748(20)	676(23)	10 909(14)
B(9)	2 962(17)	−451(19)	10 680(12)	B(10)	2 193(18)	−1 072(20)	10 398(12)
B(11)	2 291(19)	−342(21)	11 027(13)	C(31)	210(8)	3 574(12)	8 896(7)
C(32)	−172	2 764	8 735	C(33)	−803	2 688	8 849
C(34)	−1 053	3 422	9 125	C(35)	−671	4 232	9 286
C(36)	−39	4 309	9 172	C(41)	1 470(8)	4 556(10)	9 226(6)
C(42)	1 470	5 477	9 032	C(43)	1 852	6 146	9 426
C(44)	2 233	5 893	10 013	C(45)	2 233	4 972	10 207
C(46)	1 852	4 304	9 813	C(51)	805(9)	4 180(10)	7 967(5)
C(52)	233	4 725	7 715	C(53)	159	5 176	7 157
C(54)	658	5 081	6 851	C(55)	1 230	4 536	7 103
C(56)	1 304	4 085	7 661	C(61)	3 793(9)	3 900(10)	10 342(6)
C(62)	3 939	4 849	10 402	C(63)	3 970	5 302	10 952
C(64)	3 855	4 806	11 441	C(65)	3 709	3 857	11 380
C(66)	3 678	3 404	10 831	C(71)	3 692(11)	4 100(10)	9 059(6)
C(72)	4 238	4 390	8 852	C(73)	4 130	4 983	8 348
C(74)	3 474	5 286	8 052	C(75)	2 928	4 997	8 259
C(76)	3 037	4 404	8 763	C(81)	4 672(9)	2 853(12)	9 792(9)
C(82)	5 191	3 198	10 278	C(83)	5 862	2 944	10 339
C(84)	6 015	2 344	9 913	C(85)	5 496	1 998	9 427
C(86)	4 824	2 253	9 367	C(91)	2 416(9)	1 007(10)	7 823(6)
C(92)	2 113	621	7 250	C(93)	2 020	1 161	6 723
C(94)	2 232	2 087	6 770	C(95)	2 535	2 474	7 344
C(96)	2 628	1 934	7 871	C(101)	3 539(7)	147(11)	8 660(8)
C(102)	3 827	333	8 184	C(103)	4 511	142	8 256
C(104)	4 908	−235	8 804	C(105)	4 621	−422	9 280
C(106)	3 937	−231	9 208	C(111)	2 284(10)	−849(10)	8 235(7)
C(112)	2 712	−1 618	8 297	C(113)	2 443	−2 492	8 098
C(114)	1 746	−2 596	7 838	C(115)	1 318	−1 827	7 776
C(116)	1 587	−953	7 975	C(200)*	419(21)	2 428(26)	1 361(16)
Cl(1)*	245(9)	3 025(9)	1 919(7)	Cl(2)*	238(8)	3 001(8)	675(5)
C(300)*	4 532(42)	7 445(58)	2 716(36)	Cl(3)*	5 354(22)	6 988(25)	2 482(20)
Cl(4)*	3 857(35)	7 468(26)	2 128(20)				

* Solvent molecules.

hydrogen halted, the solution turned from orange to red. The mixture was then stirred at room temperature for 24 h, after which time the solvent was removed *in vacuo*. The residue was dissolved in CH_2Cl_2 (2 cm^3) and chromatographed at −30 °C. Elution with CH_2Cl_2–hexane (1:1) removed a red fraction. Solvent was removed *in vacuo* and the solid crystallised from CH_2Cl_2–hexane (10 cm^3, 1:4) to afford red *microcrystals* of **6a** (0.12 g). Further elution of the column with CH_2Cl_2–hexane (2:1) removed a yellow fraction. Solvent was removed *in vacuo*, and crystallisation of the solid from CH_2Cl_2–hexane (8 cm^3, 1:2) gave yellow *microcrystals* of $[RhAu_2(\mu\text{-}H)(PPh_3)_3(\eta^5\text{-}7,8\text{-}C_2B_9H_9Me_2)]$ **9** (0.10 g).

Synthesis of the Complex $[RhAu(PPh_3)_3(\eta^5\text{-}7,8\text{-}C_2B_9H_{11})]$.—A mixture of compounds **5c** (0.18 g, 0.25 mmol), $[RhCl(PPh_3)_3]$ (0.23 g, 0.25 mmol) and $TlBF_4$ (0.10 g, 0.34 mmol) was dissolved in thf (25 cm^3) and stirred at room temperature for 20 h. Solvent was removed *in vacuo*, and the residue was dissolved in CH_2Cl_2 (30 cm^3) and filtered through a Celite pad. The filtrate was reduced *in vacuo* to *ca.* 3 cm^3 and the solution chromatographed. Elution with CH_2Cl_2–light petroleum (1:1) removed an orange fraction. Solvent was removed *in vacuo* and crystallisation of the product from CH_2Cl_2–light petroleum (10 cm^3, 1:3) yielded orange *microcrystals* of $[RhAu(PPh_3)_3(\eta^5\text{-}7,8\text{-}C_2B_9H_{11})]$ **8b** (0.18 g).

Crystal Structure Determinations and Refinements.—The crystal data and experimental parameters for compounds **6a** and **9** are given in Table 6. Crystals of both **6a** and **9** were grown by the method of diffusion of hexane into CH_2Cl_2 solutions of the compounds. The selected crystal of compound **6a**, which crystallises with one molecule of CH_2Cl_2, was mounted in a sealed glass capillary under nitrogen. Complex **9** crystallises with two molecules of CH_2Cl_2 in the asymmetric unit, and rapid solvent loss occurs as soon as the crystals are removed from solution. The selected crystal was cut from a much larger crystal and quickly mounted in a sealed glass capillary under nitrogen saturated with CH_2Cl_2. All data were corrected for Lorentz and polarisation effects. The structures were solved by conventional heavy-atom methods, and successive Fourier difference syntheses were used to locate all non-hydrogen atoms.

For compound **6a** the data were corrected for X-ray absorption effects by an empirical method based upon azimuthal scan data.[17] The phenyl rings were refined as rigid isotropic groups, and all remaining non-hydrogen atoms were refined with anisotropic thermal parameters. The B–H→Rh hydrogen atoms H(4) and H(9) were located in a final electron-density difference synthesis, and were included in fixed positions (U_{iso} = 0.08 $Å^2$). The remaining cage B–H hydrogen atoms were included in calculated positions [B–H 1.1 Å, U_{iso} = $1.2U_{iso}$(B)].[18] Methyl and phenyl hydrogen atoms were also included in calculated positions (C–H 0.96 Å) with fixed isotropic thermal parameters (U_{iso} = 0.08 $Å^2$). The somewhat

poor quality of the data for **6a** reflects the fact that the crystals were small and diffracted weakly. In addition, the asymmetric unit contains a molecule of CH_2Cl_2, the constituent atoms of which have large anisotropic thermal parameters.

For compound **9**, during data collection three check reflections showed a progressive loss of intensity and the crystal ceased diffracting shortly after the intensity of the check reflections had decayed to *ca.* 40% of their initial values. This decay was undoubtedly associated with loss of CH_2Cl_2 from the crystal lattice, and the crystal had decomposed before data for an empirical absorption correction could be collected. Attempts to grow more tractable crystals from alternative solvents were unsuccessful. The Au, Rh, Cl and P atoms were refined with anisotropic thermal parameters. Carbon atoms were refined with isotropic thermal parameters and the phenyl rings were treated as rigid isotropic groups. The cage B–H hydrogen atoms were included in calculated positions [B–H 1.1 Å, $U_{iso} = 1.2U_{iso}(B)$],[18] as were the methyl and phenyl hydrogen atoms (C–H 0.96 Å) with fixed isotropic thermal parameters ($U_{iso} = 0.08$ Å^2). The position of the bridging Rh–H(001)–Au(1) hydrogen atom was determined from a potential-energy minimisation calculation[10] and this atom was included in a fixed position ($U_{iso} = 0.08$ Å^2). As mentioned above, the asymmetric unit contains two molecules of CH_2Cl_2. The CH_2Cl_2 molecule in the first site was given a fixed site occupancy of 1.0, but due to solvent loss the second molecule was refined with a fixed site occupancy of 0.5. Given the problems with solvent loss and decomposition of the crystal during data collection, the quality of the refinement was surprisingly good but the structural parameters for **9** should of course be treated with some caution. All computations were performed on a DEC μ-Vax II computer with the SHELXTL system of programs.[17] Scattering factors with corrections for anomalous dispersion were taken from ref. 19 and atomic coordinates are listed in Tables 7 and 8.

Additional material available from the Cambridge Crystallographic Data Centre comprises H-atom coordinates, thermal parameters, and remaining bond lengths and angles.

Acknowledgements

We thank the SERC for a research studentship (to P. A. J.), and the Robert A. Welch Foundation for support (to P. A. J. and F. G. A. S.).

References

1 (*a*) N. Carr, M. C. Gimeno, J. E. Goldberg, M. U. Pilotti, F. G. A. Stone and I. Topaloğlu, *J. Chem. Soc., Dalton Trans.*, 1990, 2253; (*b*) M. U. Pilotti, F. G. A. Stone and I. Topaloğlu, *J. Chem. Soc., Dalton Trans.*, 1991, 1355; (*c*) J. E. Goldberg and F. G. A. Stone, *Polyhedron*, 1992, **11**, 2841.
2 (*a*) J. Buchanan, E. J. M. Hamilton, D. Reed and A. J. Welch, *J. Chem. Soc., Dalton Trans.*, 1990, 677; (*b*) E. J. M. Hamilton and A. J. Welch, *Polyhedron*, 1990, **9**, 2407.
3 R. Hoffmann, *Angew. Chem., Int. Ed. Engl.*, 1982, **21**, 771.
4 K. P. Callahan and M. F. Hawthorne, *Adv. Organomet. Chem.*, 1976, **14**, 145; M. F. Hawthorne, *J. Organomet. Chem.*, 1975, **100**, 97.
5 J. A. K. Howard, J. C. Jeffery, P. A. Jelliss, T. Sommerfeld and F. G. A. Stone, *J. Chem. Soc., Chem. Commun.*, 1991, 1664.
6 J. A. Long, T. B. Marder, P. E. Behnken and M. F. Hawthorne, *J. Am. Chem. Soc.*, 1984, **106**, 2979.
7 L. W. Bateman, M. Green, K. A. Mead, R. M. Mills, I. D. Salter, F. G. A. Stone and P. Woodward, *J. Chem. Soc., Dalton Trans.*, 1983, 2599; M. Green, A. G. Orpen, I. D. Salter and F. G. A. Stone, *J. Chem. Soc., Dalton Trans.*, 1984, 2497.
8 R. R. Schrock and J. A. Osborn, *J. Am. Chem. Soc.*, 1971, **93**, 2397.
9 K. P. Hall and D. M. P. Mingos, *Prog. Inorg. Chem.*, 1984, **32**, 237.
10 A. G. Orpen, *J. Chem. Soc., Dalton Trans.*, 1980, 2509.
11 F. G. A. Stone, *Adv. Organomet. Chem.*, 1990, **31**, 53.
12 M. F. Hawthorne, D. C. Young, P. M. Garrett, D. A. Owen, S. G. Schwerin, F. N. Tebbe and P. A. Wegner, *J. Am. Chem. Soc.*, 1968, **90**, 862.
13 R. Usón and A. Laguna, *Organomet. Synth.*, 1986, **3**, 325.
14 D. Evans, J. A. Osborn and G. Wilkinson, *Inorg. Synth.*, 1968, **11**, 99.
15 J. A. Osborn and G. Wilkinson, *Inorg. Synth.*, 1967, **10**, 67.
16 R. Cramer, *Inorg. Synth.*, 1974, **15**, 17.
17 G. M. Sheldrick, SHELXTL programs for use with a Siemens X-Ray System, Cambridge, 1976; updated Göttingen, 1981.
18 P. Sherwood, BHGEN, a program for the calculation of idealised hydrogen-atom positions for a *nido*-icosahedral carbaborane fragment, Bristol University, 1986.
19 *International Tables for X-Ray Crystallography*, Kynoch Press, Birmingham, 1974, vol. 4.

Received 3rd *September* 1992; *Paper* 2/04752G